NASA TECHNICAL NOTE

NASA TN D-7335

NASA TN D-7335

A BUOYANT TORNADO-PROBE CONCEPT INCORPORATING AN INVERTED LIFTING DEVICE

by Frederick C. Grant

Langley Research Center
Hampton, Va. 23665

NATIONAL AERONAUTICS AND SPACE ADMINISTRATION • WASHINGTON, D. C. • NOVEMBER 1973

1. Report No.	2. Government Accession No.	3. Recipient's Catalog No.
NASA TN D-7335		

4. Title and Subtitle	5. Report Date
A BUOYANT TORNADO-PROBE CONCEPT INCORPORATING AN INVERTED LIFTING DEVICE	November 1973
	6. Performing Organization Code
7. Author(s)	8. Performing Organization Report No.
Frederick C. Grant	L-8969
	10. Work Unit No.
9. Performing Organization Name and Address	879-11-36-01
NASA Langley Research Center Hampton, Va. 23665	11. Contract or Grant No.
	13. Type of Report and Period Covered
12. Sponsoring Agency Name and Address	Technical Note
National Aeronautics and Space Administration Washington, D.C. 20546	14. Sponsoring Agency Code

15. Supplementary Notes

16. Abstract

Addition of an inverted lifting device to a simple balloon probe is shown to make possible low-altitude entry to tornado cores with easier launch conditions than for the simple balloon probe. Balloon-lifter combinations are particularly suitable for penetration of tornadoes with average to strong circulation, but tornadoes of less than average circulation which are inaccessible to simple balloon probes become accessible. The increased launch radius which is needed for access to tornadoes over a wide range of circulation results in entry times of about 3 minutes. For a simple balloon probe the uninflated balloon must be first dropped on, or near, the track of the tornado from a safe distance. The increase in typical launch radius from about 0.75 kilometer to slightly over 1.0 kilometer with a balloon-lifter combination suggests that a direct air launch may be feasible.

17. Key Words (Suggested by Author(s))	18. Distribution Statement
Balloons Balloon-lifter combinations Tornadoes	Unclassified – Unlimited

19. Security Classif. (of this report)	20. Security Classif. (of this page)	21. No. of Pages	22. Price*
Unclassified	Unclassified	28	Domestic, $3.00 Foreign, $5.50

*For sale by the National Technical Information Service, Springfield, Virginia 22151

A BUOYANT TORNADO-PROBE CONCEPT INCORPORATING AN INVERTED LIFTING DEVICE

By Frederick C. Grant
Langley Research Center

SUMMARY

Addition of an inverted lifting device is shown to make possible low-altitude entry to tornado cores with easier launch conditions for balloon-lifter combinations than for the simple balloon probe. Balloon-lifter combinations are particularly suitable for penetration of tornadoes with average to strong circulation, but tornadoes of less than average circulation which are inaccessible to simple balloon probes become accessible. The increased launch radius which is needed for access to tornadoes over a wide range of circulation results in entry times of about 3 minutes. For a simple balloon probe the uninflated balloon must be first dropped on, or near, the track of the tornado from a safe distance. The increase in typical launch radius from about 0.75 kilometer to slightly over 1.0 kilometer with a balloon-lifter combination suggests that a direct air launch may be feasible.

INTRODUCTION

Reference 1 describes in some detail a technique which makes possible the introduction of instrumented balloons into the cores of tornadoes by means of an airplane which, from a safe distance, parachutes the uninflated balloon on, or near, the projected track of the tornado. After the tornado has closed to some 0.75 kilometer the balloon rapidly inflates and is driven by buoyancy forces up in the gravitational field and inward in the centrifugal field of the tornado. Typical times from inflation to core entry are between 2 and 3 minutes. The self-guidance of the balloon and the safe, several-kilometer, minimum approach distance of the airplane are outstanding virtues of the technique.

Dependence on buoyancy for the driving force requires that the upward, gravity-induced buoyancy component be accepted along with the more desired inward component. Thus, a finite altitude of core entry exists for every buoyancy and launch distance. That portion of the funnel below the core-entry altitude is inaccessible to the probe. If the upward buoyancy force can be counteracted without at the same time substantially detracting from the inward buoyancy force, the entire funnel height is laid open to exploration. Furthermore, the analysis shows that entry times can be reduced with the lifter.

A simple method for counteracting the upward buoyancy is to tether an inverted lifting device below the balloon, thereby curving the flight path downward. Many forms of lifter can be envisioned such as high aspect-ratio gliders, kites of low lift-drag ratio, parawings, and low aspect-ratio gliders such as the Rogallo paraglider (ref. 2). Yet another possibility is a balloon of streamline form trimmed by tail surfaces so as to be subject to a downward aerodynamic force. This device is the limiting case of zero tether length in which buoyant and aerodynamic lift are produced by a single body. Specific results are given for the paraglider as representative of the entire class of possibilities.

The paraglider is regarded as representative only in terms of its lift and drag characteristics. Every form of lifter surely will have its own difficulties with stability, deployment, rigging, and interaction with the balloon wake. The analysis to be given produces trajectory results valid for all forms of lifter if the ancillary difficulties are assumed to be overcome.

Just as for the simple balloon, the moment of deployment of the balloon-lifter combination is the most demanding structurally. However, the deployment of the lifter can be delayed by a couple of seconds, by which time the relative wind will have diminished from gale or hurricane levels to several meters per second. (See ref. 1.)

SYMBOLS

a	lift-drag ratio of balloon-lifter combination, β/ϵ
B_r, B_z	radial and vertical components, respectively, of balloon net buoyancy force, N
B_T	resultant net buoyancy on balloon-lifter combination, N
b	tornado-strength parameter, $(\Gamma/2\pi)^2/g$, m^3
$C_{D,B}, C_{D,K}$	drag coefficients of balloon and lifter, respectively
$C_{L,K}$	lift coefficient of lifter
d	balloon diameter, m
D_B, D_K	aerodynamic drags of balloon and lifter, respectively, N
D_T	total drag of balloon-lifter combination, N
F_r, F_z, F_θ	aerodynamic forces on balloon-lifter combination in radial, vertical, and tangential directions, respectively, N

F_T	resultant aerodynamic force on balloon-lifter combination, N
g	acceleration of gravity, 9.80665 m/s^2
$I(r)$	trajectory integral over radius, m^{-2}
$k = \sqrt[3]{\frac{b}{a}}$, m	
L_K	aerodynamic lift of lifter, N
$(L/D)_K$	lift-drag ratio of lifter
m_K	mass of lifter, kg
m_T	total inertial mass of balloon-lifter combination, kg
m'	virtual mass of balloon, kg
p	atmospheric pressure, N/m^2
R_D	ratio of balloon drag to lifter drag
R_S	ratio of balloon cross-sectional area to lifter planform area
r	radial distance from tornado center, m
r_p	radius at peak altitude of trajectory, m
r_0	launch radius, m
S_B	frontal area of balloon, m^2
S_K	planform area of lifter, m^2
T	tether tension, N
t_c	time to center
v	wind speed, m/s

V_B balloon volume, m^3

v_r, v_z, v_θ velocity in radial, vertical, and tangential directions, m/s

v_{rel} relative wind, m/s

$W_{z,K}$ gravitational force on lifter, N

$W_{r,K}$ centrifugal force on lifter, N

z altitude, m

z_c altitude of probe at center, m

z_p altitude of probe at trajectory peak, m

z_ρ density scale height, 8436.1 m

$\beta = C_{L,K}S_K$, m^2

Γ tornado circulation, m^2/s

$\bar{\Gamma}$ circulation of mean tornado, 1.75×10^5 m^2/s

γ flight-path angle with horizontal, radians

$\Delta\rho_B$ balloon mass density of buoyancy, kg/m^3

$\Delta\rho_T$ total mass density of buoyancy, kg/m^3

$\epsilon = C_{D,K}S_K + C_{D,B}S_B$, m^2

θ azimuthal coordinate, radians

λ = arc tan a, radians

$\mu = \arctan \frac{v^2}{gr}$, radians

ξ, ζ radial and vertical components, respectively, of square of relative wind, m^2/s^2

ν = arc tan $(L/D)_K$, radians

ρ atmospheric density, kg/m^3

ρ_B mean mass density of balloon, kg/m^3

ρ_K equivalent density of lifter mass over balloon volume, kg/m^3

ρ_T density of total probe mass spread over balloon volume, kg/m^3

ρ_0 atmospheric mass density at sea level, 1.225 kg/m^3

ψ tether angle with vertical, radians

A dot over a symbol indicates the derivative of the quantity with respect to time.

ANALYSIS

Definition of Model

The dynamical behavior of balloon-lifter combinations is investigated for the same simple, vertical, line-vortex tornado in an isothermal atmosphere that was used in reference 1. The lifter adds five degrees of freedom to the system, two for the tether and three for the lifter, but these extra coordinates play no role in the present analysis because the lifter is assumed to ride at constant angle of attack with no sideslip, yaw, or roll. The plane of symmetry of the lifter thus always coincides with a plane through the balloon and the line vortex, and the lift and drag coefficients remain constant. The tether is assumed to lie in the plane of symmetry of the lifter and the flight-path angle is assumed the same for both balloon and lifter so that both degrees of freedom of the tether are eliminated. A view of a balloon in combination with the paraglider in flight is shown in figure 1. If the harness is so arranged that only small excursions in the intersection of the projected tie on the chord can occur, then only small changes in lift and drag coefficients can occur.

Lateral and longitudinal oscillations are neglected in the analysis because they have but a slight effect on the mean behavior. In practical cases, a lifter of low $(L/D)_K$ of, say, 4 and a sufficiently long tether between balloon and lifter should effectively inhibit the growth of small oscillations. (See ref. 3.)

Finally, in addition to numerical results, a closed form, quasi-equilibrium trajectory solution such as that of reference 1 is found. Very quickly after launch (several seconds) certain of the inertia terms of the motion equations become small compared with the other terms and may be ignored with little error. The approximation is similar to that

used in calculation of parachute trajectories (ref. 4). For parachutes, equilibrium, or terminal, speed is often used at every air density (altitude) instead of the very slightly higher actual airspeed. Such a quasi-equilibrium approximation has the great advantage of reducing the second-order motion equations to first-order equations.

As in reference 1, the tornado winds are approximated outside the core by a vertical line vortex which produces a wind speed v equal to $\Gamma/2\pi r$ for a tornado circulation Γ at a radius r. The atmospheric density is approximated by

$$\rho = \rho_0 \exp\left(-\frac{z}{z_\rho}\right)$$

for ground-level density ρ_0 and density scale height z_ρ. The corresponding vertical pressure gradient is taken as given by the barometric equation

$$\frac{\partial p}{\partial z} = -\rho g$$

where g is the acceleration of gravity. Because the Coriolis force is small compared with the centrifugal force, cyclostrophic balance is assumed in the radial direction; hence, the radial pressure gradient is

$$\frac{\partial p}{\partial r} = \frac{\rho v^2}{r}$$

The altitudes encountered during probe ascent are small enough that the exponential density approximation is adequate. The singularity at r = 0 is not a good approximation to the actual atmosphere, but use of the simple, singular vortex model does not produce significant changes in the trajectories or times to center.

Equations of Motion

The complete inhibition of lateral and longitudinal oscillations is tantamount to elimination of the several seconds of transient motion just after launch during which the probe rapidly catches up to, and then drifts with, the local tornado wind. In other words, for the tangential motion

$$r\dot{\theta} = v_\theta = v \tag{1}$$

where v_θ is the probe's tangential velocity. Equation (1) is the first-order approximate equation of motion for the azimuth angle θ. The first-order approximate equations for the radial velocity, $\dot{r} = v_r$, and the vertical velocity, $\dot{z} = v_z$, are found by suppressing the $\dot{v}_r, \dot{v}_z$ terms in the radial and vertical equations of motion.

The more exact motion equations of reference 1 included the virtual, or additional apparent, mass of the spherical balloon. When the lifter is present, corresponding equations may be written as

$$-\left(m_T + m'\right)\dot{v}_z = -\rho g V_B + m_T g + F_z \tag{2a}$$

$$-\left(m_T + m'\right)\left(\dot{v}_r - \frac{v_\theta^2}{r}\right) = \frac{\rho v^2}{r} V_B + F_r + m' \frac{v^2}{r} \tag{2b}$$

$$-\left(m_T + m'\right)\left(\dot{v}_\theta + \frac{v_r v_\theta}{r}\right) = F_\theta \tag{2c}$$

where m_T is the total mass of the balloon-lifter combination, m' is the virtual mass of the spherical balloon (half the mass of displaced fluid), and V_B is balloon volume. Only the apparent mass of the balloon appears in equations (2). For simplicity, the components of apparent mass of the lifter are omitted. The regime of validity of equations (2) is the low-acceleration period after the lifter is deployed, when the apparent mass of the balloon is assumed to dominate that of the lifter.

As mentioned previously, v_θ approximates v very closely and very quickly after launch. Because both sides of equation (2c) vanish for $v_\theta = v$, approximate equations are

$$\left(m_T + m'\right)\dot{v}_z = \Delta\rho_T g V_B - F_z \tag{3a}$$

$$\left(m_T + m'\right)\dot{v}_r = -\Delta\rho_T \frac{v^2}{r} V_B - F_r \tag{3b}$$

In equations (3) the total inertial mass of the balloon-lifter combination has been converted into an artificial density ρ_T defined by

$$\rho_T \equiv \frac{m_T}{V_B}$$

with

$$\Delta\rho_T = \rho - \rho_T$$

indicating the net density of buoyancy. Because the probe speed is up to the speed of the local wind, the additional inward force $-m' \frac{v^2}{r}$ discussed in references 1, 5, and 6 cancels against a corresponding inertial term $-m' \frac{v_\theta^2}{r}$. The final step in obtaining the quasi-equilibrium motions is to set to zero the left-hand sides of equations (3) which are small compared with terms of the right-hand sides. The forces on the spherical balloon are indicated in sketch A.

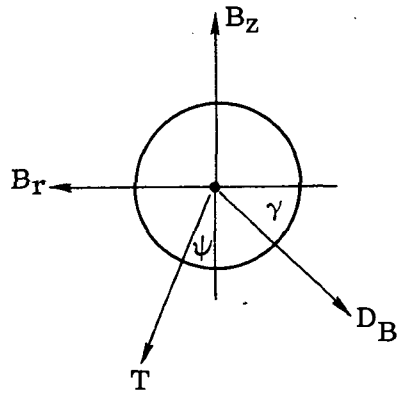

Sketch A

For motion up and to the left

$$B_r = \left(\rho - \rho_B\right)\frac{v^2}{r} V_B$$

and

$$B_z = \left(\rho - \rho_B\right) g V_B$$

are net radial and vertical buoyancies including the radial and vertical forces on the balloon in the centrifugal and gravitational fields. In sketch A, T is the tether tension, D_B is the balloon drag, γ is the flight-path angle, and ψ is the tether angle.

The forces on the lifter are shown in sketch B.

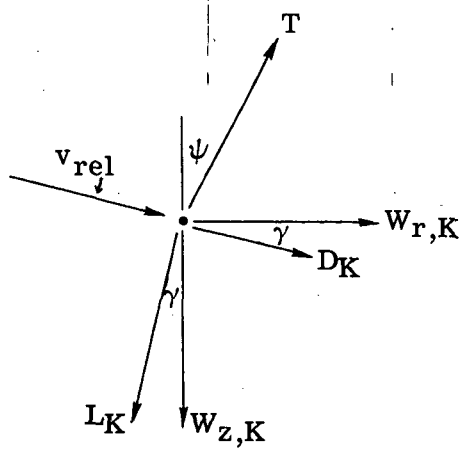

Sketch B

In sketch B, L_K and D_K are the lift and drag on the lifter, respectively; $W_{z,K}$ and $W_{r,K}$ are the forces on the lifter in the gravity and centrifugal fields, respectively.

The quasi-equilibrium equations of motion may now be written as the static equilibrium of the forces indicated in sketches A and B. For the vertical direction,

$$B_z - T \cos \psi - D_B \sin \gamma = 0 \qquad \text{(Balloon)} \qquad (4a)$$

$$T \cos \psi - W_{z,K} - D_K \sin \gamma - L_K \cos \gamma = 0 \qquad \text{(Lifter)} \qquad (4b)$$

and for the radial direction,

$$D_B \cos \gamma - T \sin \psi - B_r = 0 \qquad \text{(Balloon)} \qquad (5a)$$

$$T \sin \psi + D_K \cos \gamma - L_K \sin \gamma + W_{r,K} = 0 \qquad \text{(Lifter)} \qquad (5b)$$

By addition in each pair of equations (4) and (5), the tether tension and tether angle can be eliminated. Further simplification can be made by introducing the quantities ξ and ζ where

$$\xi = -v_{rel}^2 \cos \gamma \qquad (6a)$$

$$\zeta = v_{rel}^2 \sin \gamma \qquad (6b)$$

$$v_{rel} = \left(\xi^2 + \zeta^2\right)^{1/4} \qquad (6c)$$

and v_{rel} is the relative wind. The relative wind appears in the aerodynamic drag and lift equations:

$$D_B = \frac{1}{2} \rho v_{rel}^2 S_B C_{D,B} \qquad (7a)$$

$$D_K = \frac{1}{2} \rho v_{rel}^2 S_K C_{D,K} \qquad (7b)$$

$$L_K = \frac{1}{2} \rho v_{rel}^2 S_K C_{L,K} \qquad (7c)$$

The balloon is assumed to be spherical so that the frontal area is

$$S_B = \frac{\pi}{4} d^2$$

where d is the balloon diameter. The volume of the balloon is

$$V_B = \frac{2}{3} d S_B$$

in terms of the frontal area. No special assumptions are made for the configuration of the lifter; however, it is convenient to introduce into the equations of motion a fictitious density associated with the lifter defined by

$$\rho_K \equiv \frac{3}{2} \frac{W_{z,K}}{g d S_B}$$

This equation represents the density which the mass of the lifter would have if it were imagined to be spread uniformly over a volume equal to that of the balloon.

Introduction of the variables ξ and ζ and the aerodynamic coefficients $C_{D,B}$, $C_{D,K}$, and $C_{L,K}$ from equations (7) into the equations found by addition of equation (4a) to equation (4b) and equation (5a) to equation (5b) yields the following pair of equations:

$$-C_{L,K}S_K\xi + \left(C_{D,K}S_K + C_{D,B}S_B\right)\zeta = \frac{4}{3}\Delta\rho_T \frac{gd}{\rho} S_B \tag{8a}$$

$$\left(C_{D,K}S_K + C_{D,B}S_B\right)\xi + C_{L,K}S_K\zeta = -\frac{4}{3}\Delta\rho_T \frac{v^2}{r}\frac{d}{\rho} S_B \tag{8b}$$

in which the relative wind v_{rel} and the flight-path angle γ do not appear. The quantity $\Delta\rho_T$ is defined by

$$\Delta\rho_T \equiv \rho - \left(\rho_B + \rho_K\right) = \rho - \rho_T$$

where ρ_B is the mean density of the balloon. The altitude at which $\Delta\rho_T = 0$ is called the float altitude of the balloon. Solving equations (8) for ξ and ζ yields

$$\xi = -\frac{4}{3} S_B \frac{d}{\rho} \frac{gC_{L,K}S_K + \frac{v^2}{r}\left(C_{D,K}S_K + C_{D,B}S_B\right)}{\left(C_{D,K}S_K + C_{D,B}S_B\right)^2 + C_{L,K}^2 S_K^2} \Delta\rho_T \tag{9a}$$

$$\zeta = \frac{4}{3} S_B \frac{d}{\rho} \frac{-\frac{v^2}{r} C_{L,K}S_K + g\left(C_{D,K}S_K + C_{D,B}S_B\right)}{\left(C_{D,K}S_K + C_{D,B}S_B\right)^2 + C_{L,K}^2 S_K^2} \Delta\rho_T \tag{9b}$$

At any radius r and density ρ, equations (9) yield the quasi-equilibrium velocities and flight-path angle through

$$v_{rel} = \left(\xi^2 + \zeta^2\right)^{1/4} \tag{10a}$$

$$\dot{r} = v_r = \frac{\xi}{v_{rel}} \tag{10b}$$

$$\dot{z} = v_z = \frac{\zeta}{v_{rel}} \tag{10c}$$

$$\gamma = \tan^{-1}(-\zeta/\xi) \tag{10d}$$

The weight of the lifter appears in $\Delta\rho_T$ of equations (9) as ρ_K, an addition to the balloon density ρ_B. The balloon-lifter combination moves along its trajectory as though all the weight were in the balloon. Only the tether angle and tether tension are affected by the apportionment of weight between balloon and lifter.

The tether angle can be found by equating to zero the moments of the forces on the balloon-lifter system. Choice of moment center at the lifter yields

$$\tan \psi = \frac{2 \frac{\Delta\rho_B}{\rho} \frac{v^2}{r} + C_{D,B} S_B \xi}{2 \frac{\Delta\rho_B}{\rho} g - C_{D,B} S_B \zeta} \tag{11a}$$

for

$$\Delta\rho_B = \rho - \rho_B \tag{11b}$$

The tether tension may be found from equation (4a) as

$$T = \frac{2}{3} \rho g d S_B \left(\frac{\Delta\rho_B}{\rho} - \frac{3}{4} \frac{C_{D,B}}{gd} \zeta \right) \sec \psi \tag{12}$$

The factor to the left of the parentheses on the right-hand side of equation (12) is the weight of air displaced by the balloon; hence, the rest of the right-hand side is the tether tension in units of that weight. Equations (1), (10b), and (10c) are those equations which are numerically integrated to find the complete trajectories and entry times.

Closed-Form Trajectories

In the limit of no lifter $\left(S_K = W_K = 0\right)$, equations (9) reduce to

$$\xi = -\frac{4}{3} \frac{\Delta\rho_B}{\rho} \frac{v^2}{r} \frac{d}{C_{D,B}} \tag{13a}$$

$$\zeta = \frac{4}{3} \frac{\Delta\rho_B}{\rho} g \frac{d}{C_{D,B}} \tag{13b}$$

The ratio of equation (13b) to (13a) is

$$\frac{\zeta}{\xi} = \frac{\dot{z}}{\dot{r}} = \frac{dz}{dr} = -\frac{gr}{v^2} = -g\left(\frac{2\pi}{\Gamma}\right)^2 r^3 \tag{14a}$$

or

$$-r^3 = \frac{1}{g}\left(\frac{\Gamma}{2\pi}\right)^2 \frac{dz}{dr} \tag{14b}$$

Equation (14b) is the balloon trajectory equation of reference 1. Similarly, the ratio of equation (9b) to (9a) yields

$$-\frac{dz}{dr} = \frac{-\frac{v^2}{r}\beta + g\epsilon}{g\beta + \frac{v^2}{r}\epsilon} \tag{15a}$$

where

$$\beta = C_{L,K} S_K$$

$$\epsilon = C_{D,K} S_K + C_{D,B} S_B$$

Independence of the trajectories from $\Delta\rho_T$ shows, as in the nonlifting condition, that only the time of traverse depends on $\Delta\rho_T$, to which the driving force (buoyancy) is proportional. Introduction of the lift-drag ratio of the balloon-lifter combination

$$a = \frac{\beta}{\epsilon} = \frac{C_{L,K}S_K}{C_{D,K}S_K + C_{D,B}S_B} \tag{15b}$$

and the tornado-strength parameter

$$b = \frac{1}{g}\left(\frac{\Gamma}{2\pi}\right)^2 \tag{15c}$$

where $v = \Gamma/2\pi r$ has been used, yields

$$-\int dz = -ab \int \frac{dr}{b + ar^3} + \int \frac{r^3 dr}{b + ar^3} \tag{15d}$$

where the parameter a is a measure of the effectiveness of the balloon-lifter combination in curving downward the trajectory and b is a measure of the relative strengths of the radial and vertical buoyancies. Specifically, b is the ratio, at unit distance from the vortex, of radial to vertical buoyancies. The integrals on the right-hand side of equation (15d) are elementary and quadrature yields

$$z = \frac{r_0 - r}{a} - \left(ab + \frac{b}{a}\right)\left[I(r_0) - I(r)\right] \tag{16a}$$

for

$$I(r) = \frac{k}{b}\left\{\frac{1}{6}\log\left[\frac{(r + k)^2}{r^2 - kr + k^2}\right] + \frac{1}{\sqrt{3}}\tan^{-1}\left(\frac{r\sqrt{3}}{2k - r}\right)\right\} \tag{16b}$$

where

$$k = \left(\frac{b}{a}\right)^{1/3} = \left[\frac{1}{g}\left(\frac{\Gamma}{2\pi}\right)^2 \frac{C_{D,K}S_K + C_{D,B}S_B}{C_{L,K}S_K}\right]^{1/3} \tag{16c}$$

Altitude Peak

Equation (15a) yields a simple result when the left-hand side is set to zero. A peak is found in the trajectory (as viewed in the moving plane of the balloon and line vortex) when

$$r_p = (ab)^{1/3} = \left[\frac{1}{g}\left(\frac{\Gamma}{2\pi}\right)^2 \frac{C_{L,K}S_K}{C_{D,K}S_K + C_{D,B}S_B}\right]^{1/3} \tag{17}$$

The trajectories with lift have the form shown by the solid line in sketch C.

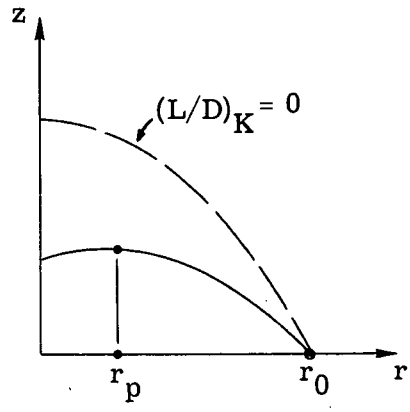

Sketch C

As the balloon without lift rises along the dotted line, its motion is first dominated by the nearly constant vertical buoyancy and then by the radial buoyancy which increases with the diminishing radius. Peak altitude is at the center, r = 0. As expected, addition of downward lift impedes the upward motion by curving the trajectory downward. At the same time the gradually increasing relative wind caused by the increasing radial buoyancy produces lift which increases as the square of the relative wind. The lift becomes so strong that eventually the flight path points downward all the way to the center. Inside of r_p both radial buoyancy and lift are important.

Although the balloon is descending after passing point p, it can be easily shown that the pressure is a monotonic decreasing function of time

$$\dot{p} = \rho g \dot{r} \left(\frac{1 + \frac{b^2}{r^6}}{a + \frac{b}{r^3}} \right) < 0$$

Thus, the balloon remains taut throughout the trajectory and maintains constant volume.

Force Balance on Balloon-Lifter Combination

From equations (9) and (10a), the relative wind v_{rel} after algebraic manipulations becomes

$$v_{rel} = \sqrt{\frac{4}{3} \frac{S_B g d}{C_{D,K} S_K + C_{D,B} S_B} \frac{\Delta\rho_T}{\rho}} \left(\frac{1 + \frac{b^2}{r^6}}{1 + a^2} \right)^{1/4} \tag{18}$$

Equation (18) can be regarded as a statement of the balance of the total aerodynamic force F_T and total net buoyancy B_T. By substitution in the numerator and denominator under the square root in equation (18) with the net vertical buoyancy B_Z and total drag of the balloon-lifter combination D_T, equation (18) becomes on squaring and rearranging

$$\left(1 + a^2\right)^{1/2} D_T = B_Z \left(1 + \frac{b^2}{r^6}\right)^{1/2} \tag{19}$$

The half-power factors in equation (19) are the secants of the angles between total drag and total aerodynamic force and between vertical buoyancy and total buoyancy. Thus, equation (19) can be written

$$F_T = B_T \tag{20}$$

Equation (20) and the definitions of lift and drag allow the immediate construction of the vector diagram of the external (no tether tension) forces on the balloon-lifter combination shown in figure 2.

The motion equations (10b) and (10c) may be rewritten, by use of equations (9), (15b), and (15c) as

$$\dot{r} = \frac{\xi}{v_{rel}} = -\frac{v_{rel}}{\sqrt{\left(1 + a^2\right)\left(1 + \frac{b^2}{r^6}\right)}}\left(a + \frac{b}{r^3}\right) \tag{21}$$

and

$$\dot{z} = \frac{\zeta}{v_{rel}} = \frac{v_{rel}}{\sqrt{\left(1 + a^2\right)\left(1 + \frac{b^2}{r^6}\right)}}\left(1 - \frac{ab}{r^3}\right) \tag{22}$$

As may be seen in equation (22), the peak altitude occurs at radius $r_p = \sqrt[3]{ab}$ of the trajectory inside of which the lift and radial buoyancy dominate the motion. From equation (21) the corresponding $\dot{r}$ is seen to be $-\left(v_{rel}\right)_p$ as expected.

Squaring of equation (18) and substitution of $r_p = (ab)^{1/3}$ shows the dynamic pressure at the peak altitude to be

$$\left(\frac{1}{2}\rho v_{rel}^2\right)_p = \frac{2}{3}\frac{S_B g d}{C_{D,B}S_B + C_{D,K}S_K}\left(\Delta\rho_T\right)_p \frac{1}{a}$$

which for a given lifter is independent of tornado strength b except through $\Delta\rho_T$. However, $\Delta\rho_T$ varies only slightly for practical cases in which the changes in peak altitude over a range of tornado strength are a small fraction of the density scale height and of the float altitude.

RESULTS

Limitations on Lift Parameter a

The motion of the balloon-lifter combination depends on a parameter a additional to the tornado-strength parameter b. The form of the parameter a is

$$a = \frac{(L/D)_K}{1 + R_D}$$

where

$$R_D = \frac{C_{D,B}S_B}{C_{D,K}S_K}$$

In addition to the aerodynamic efficiency of the lifter $\left(\text{lift-drag ratio } (L/D)_K\right)$, the ratio R_D of ballistic parameters appears.

In most of the trajectory calculations to follow, representative values of the aerodynamic coefficients are assumed. That is, $C_{D,B}$, $(L/D)_K$, and $C_{D,K}$ are held constant and $R_S = S_B/S_K$ is varied. The values of a for arbitrary $(L/D)_K$ and R_D are plotted in figure 3.

Although the range of a in figure 3 is arbitrary, an upper limit to a must be respected at every launch radius. For increasingly large lifting capability the flight path will curve increasingly downward and for sufficiently large a-values the probe will crash short of the center. The limiting case is the one for which the probe crashes exactly at the center. By iteration in the trajectory equations (16), the limiting values of a have been calculated for a large number of cases and the results are plotted in figure 4. The three curves correspond to weak, average, and strong tornadoes (ref. 7). It may be fairly concluded from figure 4 that for launches inside of a kilometer an a-value no greater than about 1 is needed for strong and average tornadoes, and an a-value no greater than about 2 is needed for weak tornadoes. Such small values correspond to weak lifting devices. It should be remembered that for given aerodynamic qualities of a lifter, the value of a can be reduced simply by reducing the size of the lifter $\left(\text{increasing } R_S = S_B/S_K\right)$.

The upper values of a given in figure 4 indicate another limit on the performance of the balloon-lifter combination, the minimum volume in which the probe can operate from a fixed launch radius. This limit is defined by the altitude of the peak of the arch in the probe-vortex plane for the limiting a-values of figure 4. The position of the peaks for the three tornado strengths of figure 4 are shown in figure 5. For launches within a kilometer radius, probes making zero-altitude entry do not rise over about 0.3 km at any tornado strength. The containment power of even weak lifters is thus demonstrated.

Fixed-Geometry Probes

The results shown in figures 4 and 5 define interesting limits, but every point on every curve corresponds to a different value of a, hence to a different balloon-lifter combination. It is natural to consider now the performance of specific vehicles at different launch radii over the range of tornado strengths.

The balloon considered is the same 2-meter-diameter, hydrogen-filled balloon considered in reference 1 with $C_{D,B} = 0.4$. The lifter might be the Rogallo parawing whose aerodynamic characteristics may be found in reference 2. The parawing is but one example of many aerodynamically equivalent configurations. At high angles of attack the $(L/D)_K$ of a parawing approaches zero as it does for any wing. As the angle of attack is reduced, the lift coefficient rises to a value of about 0.4 at a drag coefficient of 0.1. Although a rigid Rogallo configuration attains higher $(L/D)_K$ values at lower angles of attack, a fabric configuration begins to luff (flap at the trailing edge). Values corresponding to the onset of luffing will be used. In addition to the hydrogen mass of the balloon, a mass of 1.6 kilograms is assumed in the lifter. Results for other masses are easily scaled. In practice, helium is the gas of choice; hydrogen is used in the calculations to define the ultimate probe performance. Use of helium results in a small decrease of buoyancy, 7.4 percent.

Vehicles of different lifting capability can be studied by using different values of $R_S = S_B/S_K$. An infinite value of R_S corresponds to a vanishingly small lifter. Finite values of R_S corresponds to different relative sizes of balloon and lifter. The largest lifter to be considered is one with the same area as the balloon, $R_S = 1.0$. The calculated heights at center for launch radii between 0.6 and 1.0 km in weak, average, and strong tornadoes are shown in figure 6.

Nearly all of the compromises involved in choosing a size for the lifter can be discussed in terms of figure 6. If it is desired to have the probe arrive at the core under the lowest cloud base, it must arrive at an altitude of no more than 0.3 km. For average conditions (fig. 6(b)) the base is at about 0.95 km, while the highest base is off the plot at about 1.5 km. For a weak tornado $R_S \approx 2$ is required for entry at average base height when launch is at a radius of 0.8 km. Correspondingly, $R_S \approx 16$ suffices for an average tornado and even a balloon alone $(R_S = \infty)$ will enter below the average base height in a strong tornado. Under a more stringent requirement that entry be made below the lowest cloud base, not even $R_S = 1$ suffices for a weak tornado while figure 6(c) shows that a balloon-lifter combination with $R_S = 1$ will crash in a strong tornado when launched at 0.8 km. The conflict might be stated as: Large lifters and small launch radii for weak tornadoes as opposed to small lifters and large launch radii for strong tornadoes.

A better approach might well be to abandon the weak tornadoes and to concentrate on low-altitude entry to average and strong tornadoes. Certainly, average and strong

tornadoes are more suitable subjects of study because of their more destructive character. Accordingly, selection of a moderate value, say $R_S = 4$, at a launch radius of 0.8 km might be considered. Such a probe would provide core entry at 0.2 to 0.6 km for average to strong tornadoes. The trajectories corresponding to $R_S = 4$ and launch at 0.8 km as observed in the moving probe-vortex plane are shown in figure 7. Viewed from above in ground-fixed coordinates the paths of the probes are always smooth spirals of constantly diminishing radius. Along the spirals, in the model assumed, the velocity perpendicular to the vortex-probe radius is always equal to that of the wind.

The powerful effect of the lifter is evident in figure 7. Without lift in a weak tornado, the balloon alone will not ever reach the center because it comes up to its float altitude of 9 km first. With lift, it reaches the center in less than 6 minutes some 0.2 km above the maximum cloud base of 1.5 km. The time is longer and the arrival higher but is a great improvement nonetheless. The performance in the average tornado improves from arrival without the lifter at 1.3 km altitude in 3 minutes 25 seconds to arrival with the lifter at 0.6 km in 2 minutes 20 seconds. Less marked improvement occurs in the strong tornado, but the performance in a strong tornado is sufficiently impressive without a lifter.

Launch Conditions

At this point another influence on the choice of vehicle may be introduced; namely, the wind speed at launch. For the three cases presented in figure 7 which span the range of tornado strength, the tornado winds at a radius of 0.8 km are 12, 35, and 58 meters per second, respectively. The winds are thus hurricane force for the average tornado and about 209 km per hour (130 mph) for the strong tornado. Without experiments one cannot be dogmatic. However, although rapid inflation can very likely be brought off successfully in hurricane winds (ref. 8), it seems likely that ground launches in 209-km-per-hour (130-mph) winds will prove very much more difficult. Dynamic pressures are nearly three times as high in the strong tornado as in the average tornado at 0.8-km launch radius. Air launches of balloons have been successful at speeds over 161 km per hour (100 mph) (ref. 9).

If sufficiently favorable launch conditions are maintained while at the same time a low entry height at the core is provided, the necessary change in parameters is plain: larger lifters and larger launch radii are needed. Consider what can be regarded as a shift to a very large launch radius and a very large lifter: $r_0 = 1.1$ km and $R_S = 1$. The trajectories corresponding to these values are indicated in figure 8 in the same manner as are those in figure 7.

With such a large lifter the center is reached below the mean cloud base height even in the weak tornado. In the strong tornado the probe crashes just short of the center.

Launch winds are 31, 90, and 150 km per hour (19, 56, and 94 mph) for weak, average, and strong tornadoes, respectively.

Release of Lifter

The crash indicated in figure 8 is a reminder that the core entry portion has been heretofore somewhat neglected as compared with the rest of the entry trajectory. At some point the lifter must be cut loose from the balloon so that a better response to the central winds of the tornado can be achieved. Although a somewhat arbitrary choice, the point of highest altitude seems appropriate. It marks the place where the lifter overcomes the vertical buoyancy and is near, but not in, the core. It happens that the peak altitude occurs at very nearly the same value of the dynamic pressure in the model tornadoes considered so that, for example, a flat plate drag sensor on the lifter will provide self-timing for cutting of the tether. The change in the trajectories resulting from cutting of the tether at peak altitude is indicated in figure 8. Because the probe is near the center, the times are not much affected (shortened slightly) but the steep descents (and the crash) are eliminated.

Times to Center

The times to center for a wide range of lifter size (the largest with $R_S = 1$ and the smallest with $R_S = 16$) are shown in figure 9. Some features in figure 9 should first be mentioned. In the weak tornado the probe with the smallest lifter is not captured in less than 10 minutes for radii slightly greater than 0.7 km, which is why only a single point is shown. The other extreme behavior, a crash short of center, first occurs in the average tornado for the large lifter at a launch radius of about 0.8 km, which is why the $R_S = 1$ curve is cut short. In the strong tornado, the large lifter crashes for all radii inside about 1.1 km; hence, only a single point is shown for $R_S = 1$. In general, the times to center increase rapidly with launch radius, particularly for the smaller lifters. As with the desire for low-altitude entry, the desire for fast entry to the core conflicts with the need for acceptable launch conditions. Furthermore, if entry times are not to be far from, say, 3 minutes for a range from slightly below average tornado strength to the strongest tornado strength, then the largest lifters should be used.

The times given in figure 9 are for a relatively light probe ($\Delta\rho_T = 0.86$ kg/m^3), but the times in figure 9 can be easily scaled. The relative wind varies as $\sqrt{\Delta\rho_T}$. Since the probe traverses the same trajectory if only the weight is changed (eqs. (15)), the time of passage varies as $1/\sqrt{\Delta\rho_T}$.

CONCLUDING REMARKS

Addition of an inverted, rapidly deployed, lifting device to the rapidly inflated balloon tornado probe makes possible low-altitude entry to tornado cores with easier launch conditions than the balloon alone. Balloon-lifter combinations are particularly suited to penetration of tornadoes with average to strong circulations. Although for the same launch conditions the time to center is shortened by the lifter, compromises made to provide easier launch conditions and access to tornadoes over a wide range of tornado strength leave the entry times in the neighborhood of 3 minutes. On the other hand, these same compromises increase the launch radius from about 0.75 kilometer to about a kilometer and suggest that an air launch of the balloon-lifter probe may be feasible.

Langley Research Center,
National Aeronautics and Space Administration,
Hampton, Va., July 31, 1973.

REFERENCES

1. Grant, Frederick, C.: Proposed Technique for Launching Instrumented Balloons Into Tornadoes. NASA TN D-6503, 1971.

2. Rogallo, Francis Melvin; Lowry, John G.; Croom, Delwin R.; and Taylor, Robert T.: Preliminary Investigation of a Paraglider. NASA TN D-443, 1960.

3. Söhne, W.: Directional Stability of Towed Airplanes. (Die Seitenstabilität eines geschleppten Flugzeuges.) NACA TM 1401, 1956. (Translated from Deut. Ing.-Arch., vol. 21, no. 4, 1953, pp. 245-265.)

4. Webster, A. P.: Free-Falls and Parachute Descents in the Standard Atmosphere. NACA TN 1315, 1947.

5. Taylor, Geoffrey Ingram: The Forces on a Body Placed in a Curved or Converging Stream of Fluid. Proc. Roy. Soc. (London), ser. A, vol. CXX, 1928, pp. 260-283.

6. Kelvin (Lord): On the Motion of Rigid Solids in a Liquid Circulating Irrotationally Through Perforations in Them or in a Fixed Solid. Phil. Mag., vol. XLV, 1873, pp. 332-345.

7. Chang, C. C.: Recent Laboratory Model Study of Tornadoes. Preprints of Papers Presented at the Sixth Conference on Severe Local Storms, Amer. Meteorol. Soc., Apr. 1969, pp. 244-252.

8. Steinberg, Sy; and Holle, Glenn F.: Experimental Results of the Deployment/Rapid Inflation Characteristics of a Buoyant Venus Station Balloon. Paper No. 69-1017, Collection of Technical Papers, AIAA/ASTM/IES 4th Space Simulation Conference, Sept. 1969.

9. Booker, D. Ray; and Cooper, Lynn, W.: Superpressure Balloons for Weather Research. J. Appl. Meteorol., vol. 4, no. 1, Feb. 1965, pp. 122-129.

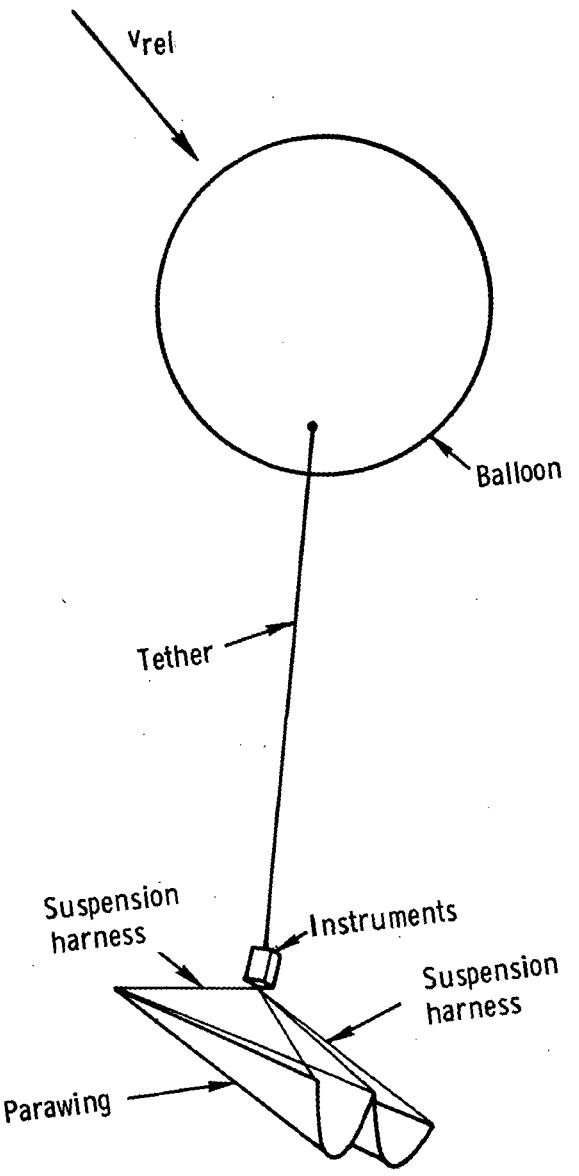

Figure 1.- View of balloon-lifter combination in flight.

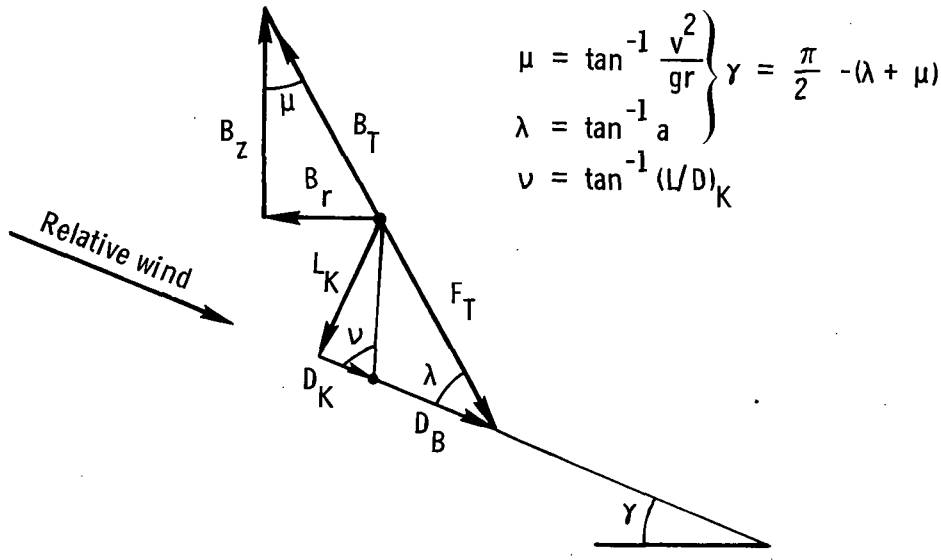

Figure 2.- Quasi-equilibrium of external forces on balloon-lifter combination.

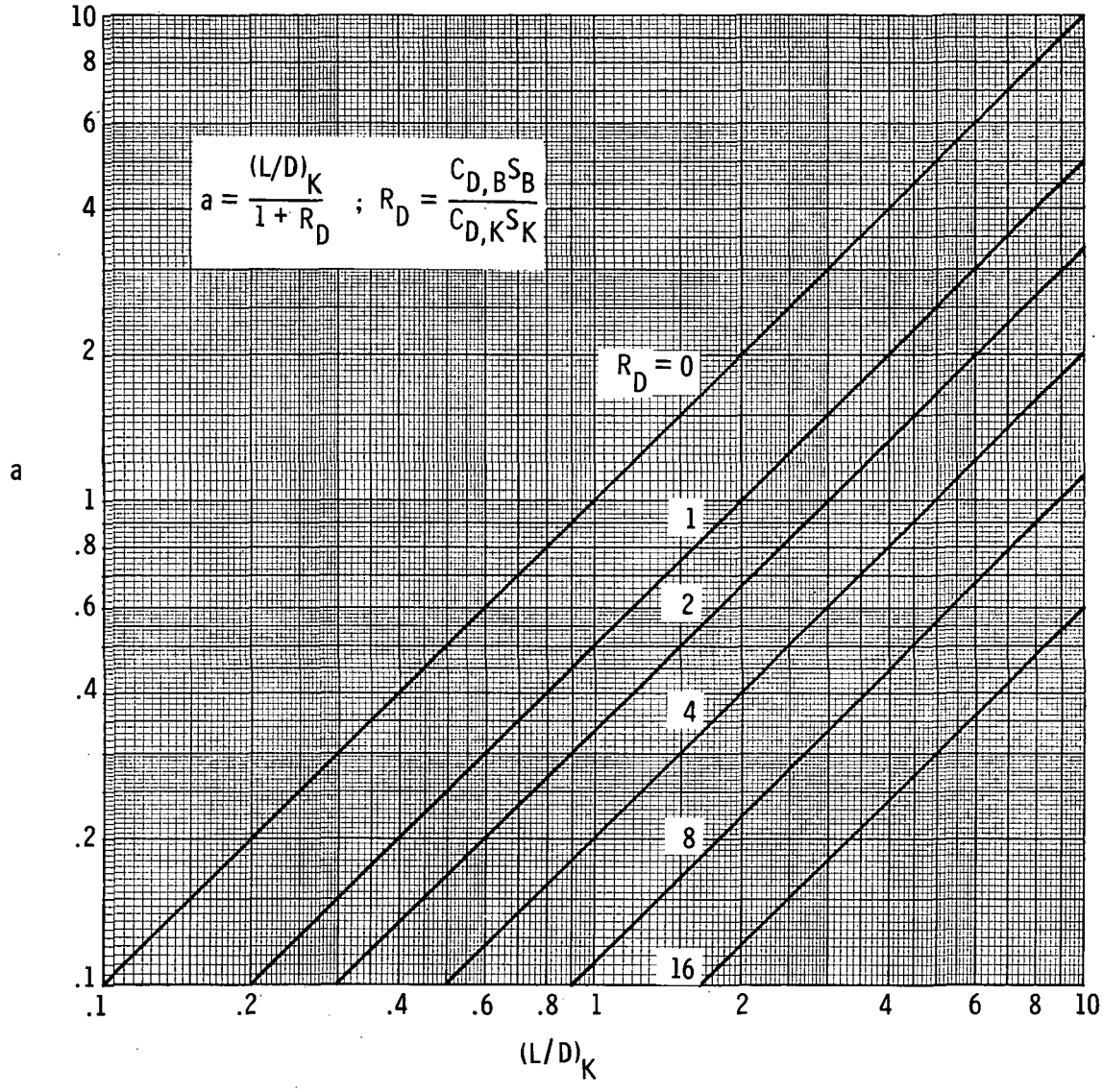

Figure 3.- Variation of a of balloon-lifter tornado probe as a function of lifter $(L/D)_K$.

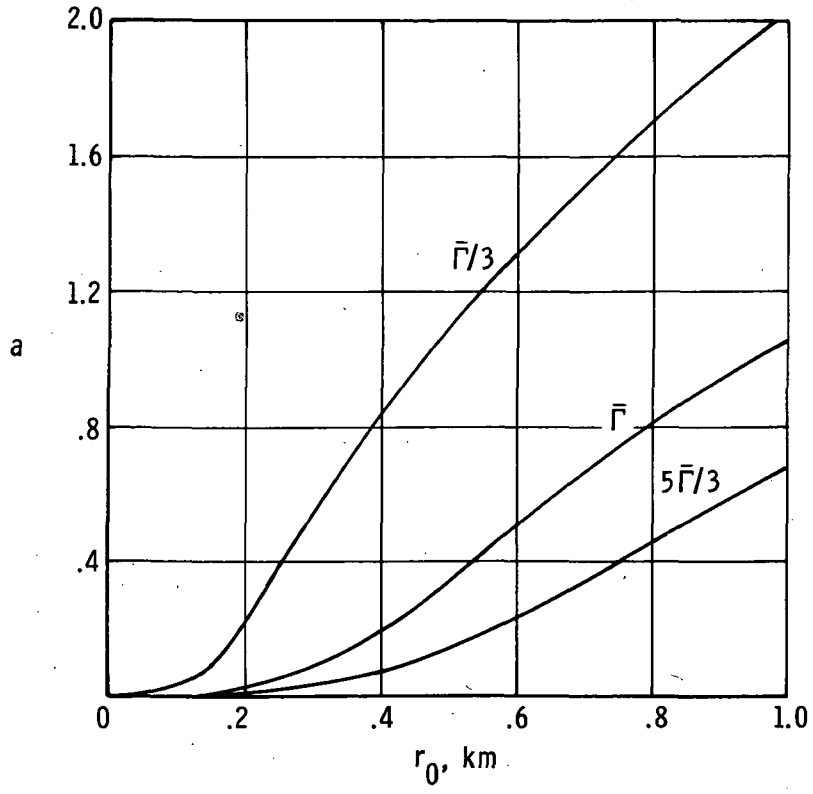

Figure 4.- Lift parameter a for zero altitude entry as a function of launch radius r_0.

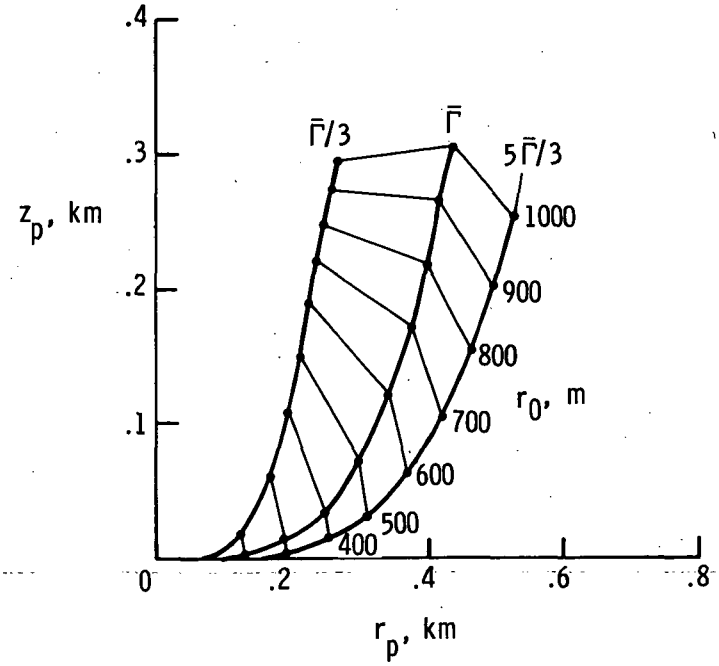

Figure 5.- Altitudes and radii of trajectory peaks for different launch radii r_0.

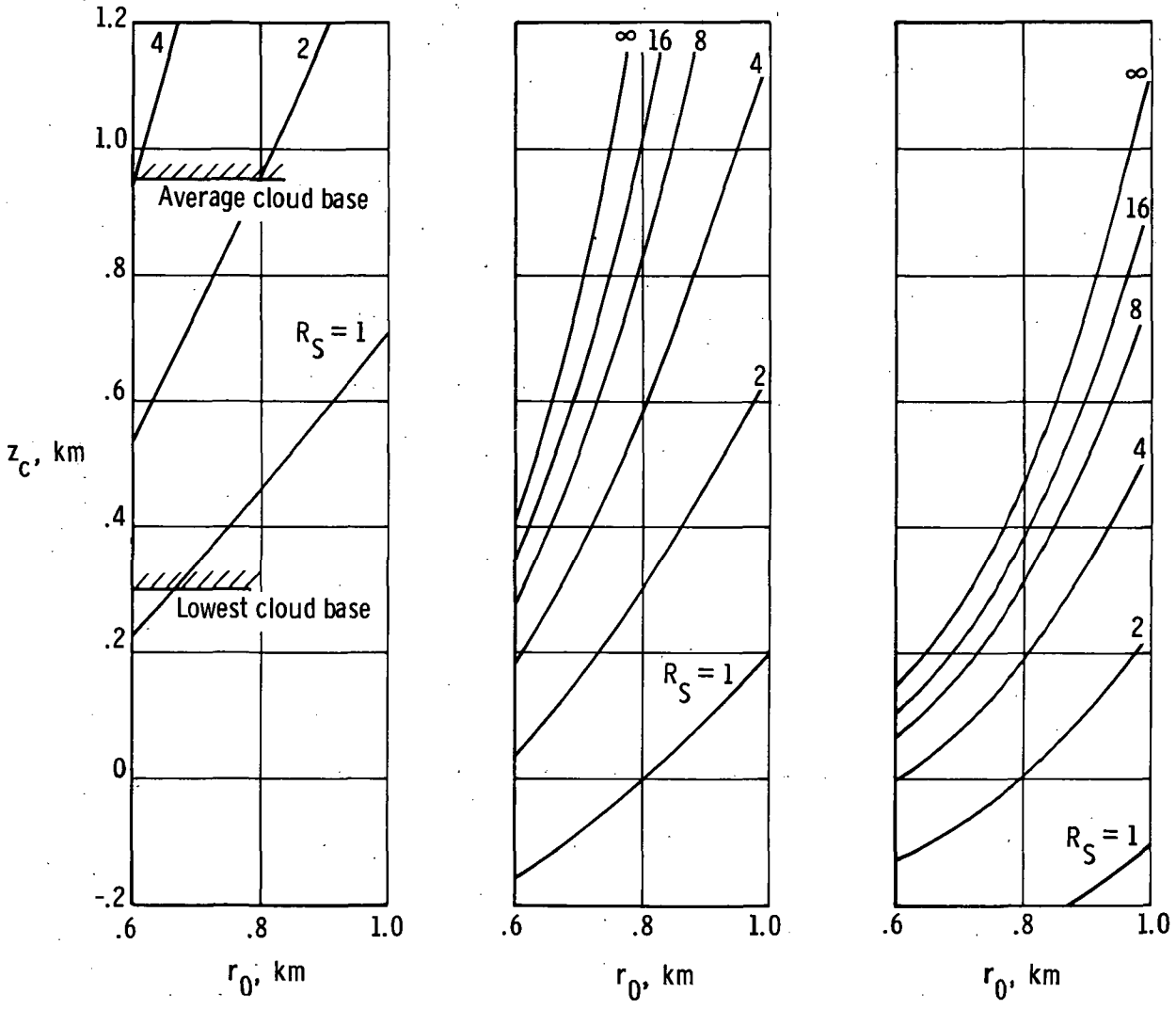

(a) Weak tornado, $\overline{\Gamma}/3$. (b) Average tornado, $\overline{\Gamma}$. (c) Strong tornado, $5\overline{\Gamma}/3$.

Figure 6.- Height at center as a function of launch radius. $C_{L,K} = C_{D,B} = 0.4$; $(L/D)_K = 4.0$; d = 2.0 m; $m_K = 1.6$ kg; $\rho_B = 0.0845$ kg/m^3; $\overline{\Gamma} = 1.75 \times 10^5$ m^2/s.

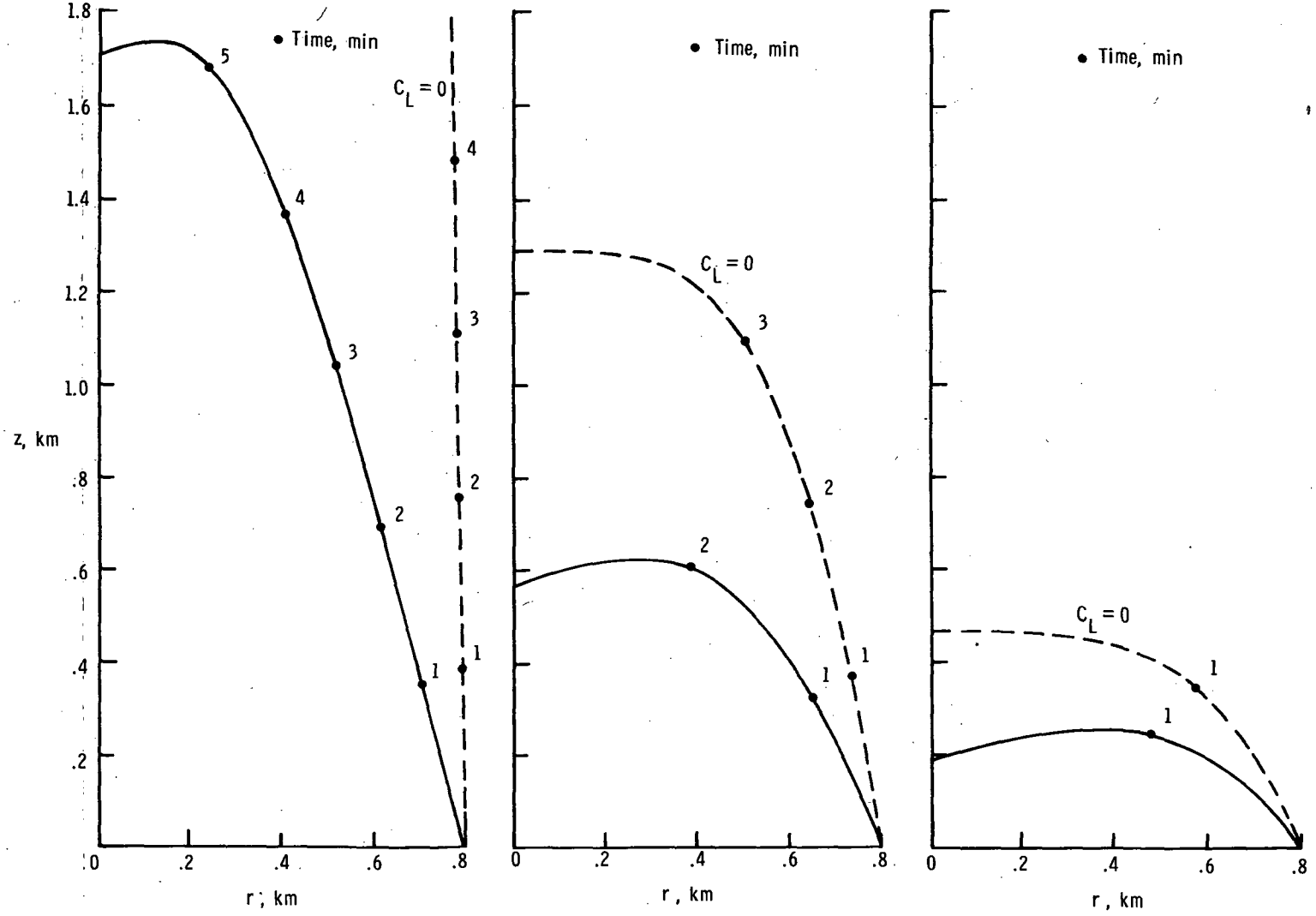

(a) Weak tornado, $\overline{\Gamma}/3$. (b) Average tornado, $\overline{\Gamma}$. (c) Strong tornado, $5\overline{\Gamma}/3$.

Figure 7.- Trajectory in moving plane of balloon-lifter combination and vortex for a wide range of tornado strength and for moderate and zero lifter size. $C_{L,K} = C_{D,B} = 0.4$; $(L/D)_K = 4.0$; d = 2.0 m; $m_K = 1.6$ kg; $\rho_B = 0.0845$ kg/m^3.

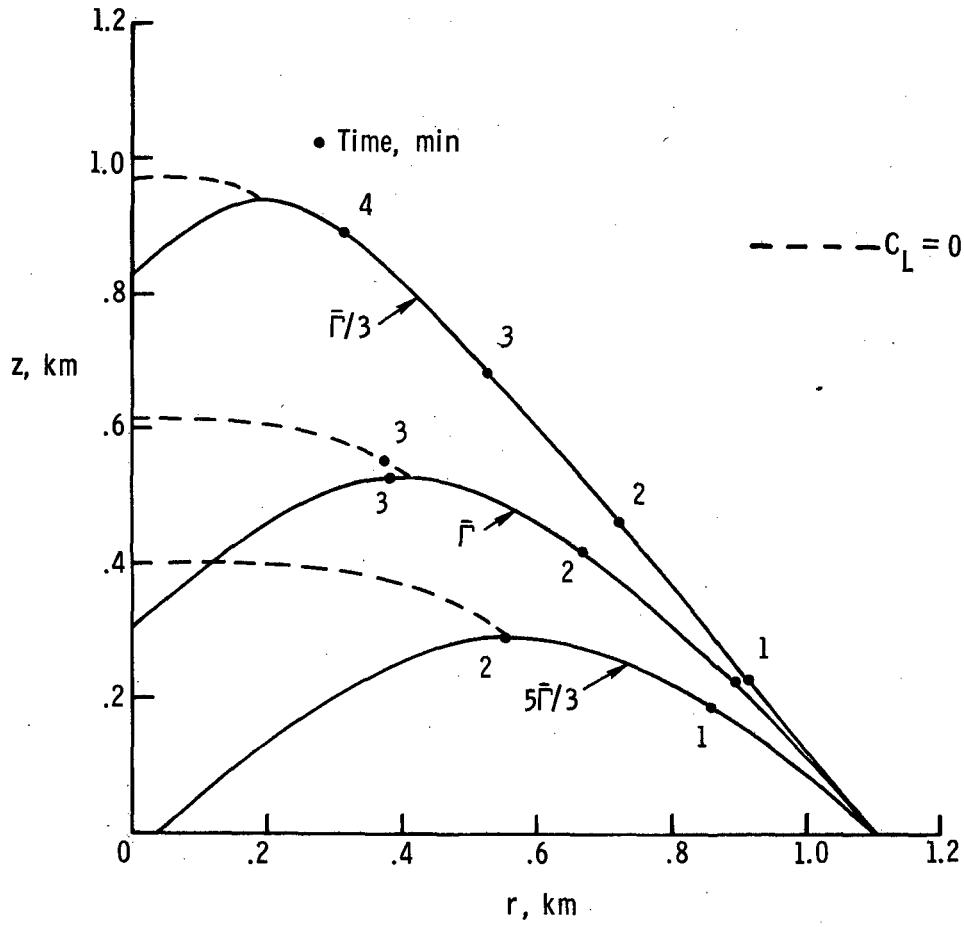

Figure 8.- Trajectories in moving plane of balloon-lifter combination and vortex for a large lifter at a large launch radius. $R_S = 1.0$; $C_{L,K} = C_{D,B} = 0.4$; $(L/D)_K = 4.0$; $d = 2.0$ m; $m_K = 1.6$ kg; $\rho_B = 0.0845$ kg/m^3.

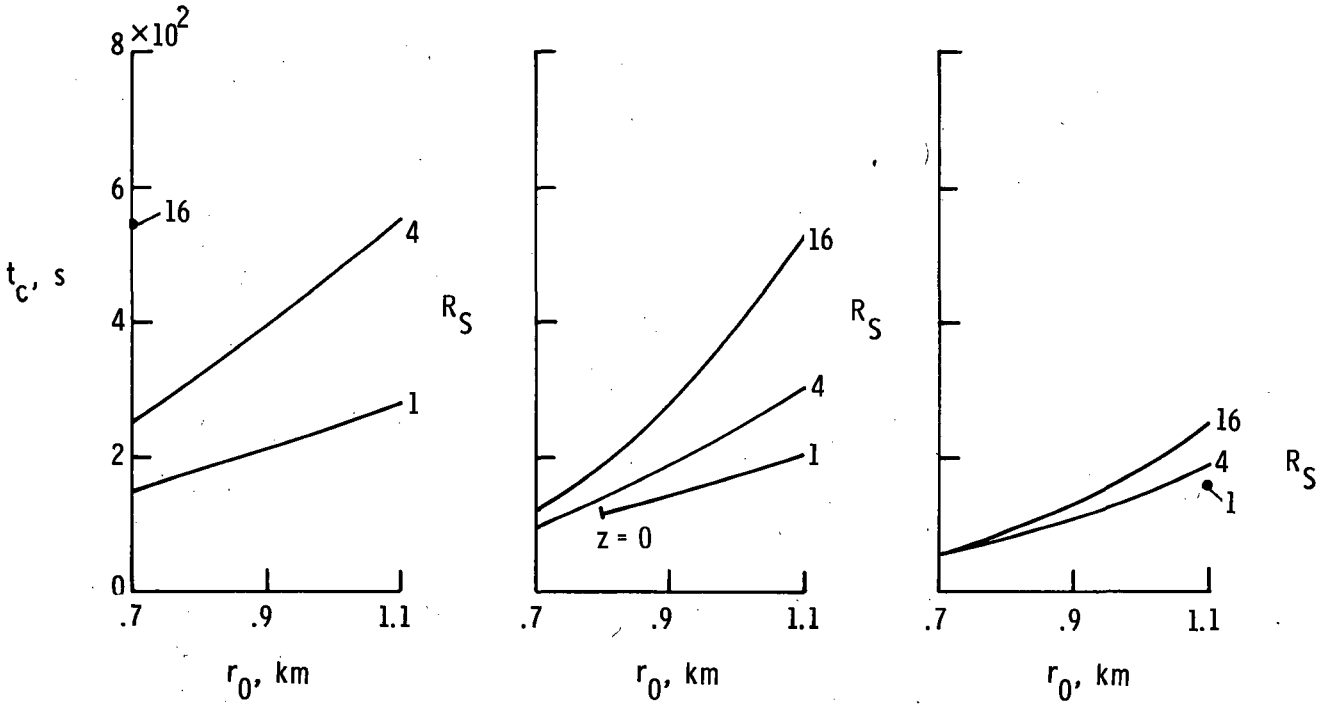

(a) Weak tornado, $\overline{\Gamma}/3$. (b) Average tornado, $\overline{\Gamma}$. (c) Strong tornado, $5\overline{\Gamma}/3$.

Figure 9.- Entry times for probes of different lifting capabilities. $C_{L,K} = C_{D,B} = 0.4$; $(L/D)_K = 4.0$; $d = 2.0$ m; $m_K = 1.6$ kg; $\rho_B = 0.0845$ kg/m^3; $\Delta\rho_T = 0.86$ kg/m^3.

NATIONAL AERONAUTICS AND SPACE ADMINISTRATION
WASHINGTON, D.C. 20546

OFFICIAL BUSINESS
PENALTY FOR PRIVATE USE $300

SPECIAL FOURTH-CLASS RATE BOOK

POSTAGE AND FEES PAID
NATIONAL AERONAUTICS AND SPACE ADMINISTRATION
451

U.S.MAIL

POSTMASTER: If Undeliverable (Section 158 Postal Manual) Do Not Return

"The aeronautical and space activities of the United States shall be conducted so as to contribute . . . to the expansion of human knowledge of phenomena in the atmosphere and space. The Administration shall provide for the widest practicable and appropriate dissemination of information concerning its activities and the results thereof."

—NATIONAL AERONAUTICS AND SPACE ACT OF 1958

NASA SCIENTIFIC AND TECHNICAL PUBLICATIONS

TECHNICAL REPORTS: Scientific and technical information considered important, complete, and a lasting contribution to existing knowledge.

TECHNICAL NOTES: Information less broad in scope but nevertheless of importance as a contribution to existing knowledge.

TECHNICAL MEMORANDUMS: Information receiving limited distribution because of preliminary data, security classification, or other reasons. Also includes conference proceedings with either limited or unlimited distribution.

CONTRACTOR REPORTS: Scientific and technical information generated under a NASA contract or grant and considered an important contribution to existing knowledge.

TECHNICAL TRANSLATIONS: Information published in a foreign language considered to merit NASA distribution in English.

SPECIAL PUBLICATIONS: Information derived from or of value to NASA activities. Publications include final reports of major projects, monographs, data compilations, handbooks, sourcebooks, and special bibliographies.

TECHNOLOGY UTILIZATION PUBLICATIONS: Information on technology used by NASA that may be of particular interest in commercial and other non-aerospace applications. Publications include Tech Briefs, Technology Utilization Reports and Technology Surveys.

Details on the availability of these publications may be obtained from:

SCIENTIFIC AND TECHNICAL INFORMATION OFFICE

NATIONAL AERONAUTICS AND SPACE ADMINISTRATION

Washington, D.C. 20546